A survey for variable young stars with small telescopes: IX - Evolution of Spot Properties on YSOs in IC 5070

Herbert et al. 2024

Helong Guo (郭贺龙，hlguo@ynu.edu.cn)

Yunnan University

2024-3-29

Introduction

- Young Stellar Objects (YSOs) display variability on a wide range of timescales. Rotational modulation caused by surface spots occurs when spots rotate in and out of the observer’s line of sight.
- The fast rotation of young stars hence results in photometric variability on the order of days. The amplitude of variation produced by spots depends on the nature and the characteristics of the spot.
- Cold spots are regions on the photosphere, analogous to sun spots, that are hundreds of degrees cooler than the stellar temperature.
- Hot spots are considered to be footprints of accretion with temperatures that are several thousand degrees above the stellar temperature and coverage less than a few percent of the stellar surface.
- Cold spots are expected to be present during all stages of the pre-main sequence evolution of stars, whereas hot spots are thought to be exclusive to accreting classical T Tauri (stage 2) stars with full or transition discs.
- However, recent surveys present a more diverse picture with low temperature contrast, high coverage regions.

HOYS data and photometry

- HOYS (Hunting Outbursting Young Stars) is a citizen science project (Froebrich et al. 2018). This uses a world wide network of ≈ 100 amateur, university, and professional telescopes to conduct long term photometric monitoring of 25 nearby (d < 1 kpc) young clusters and star forming regions in optical broad band filters.
- The aim of this project is to obtain photometry in all filters for all target regions with a cadence of 12 – 24 hours over many years.
- The photometry is calibrated against reference images taken under photometric conditions in u, B, V, R C , and I C filters (simplicity, refer to them as U, B, V, R, and I).
- To account for colour terms in the calibration due to instrumentation (e.g. slightly non-standard filters) or conditions (e.g. cirrus clouds), an internal calibration is applied to all data following Evitts et al. (2020).
    - ➢ They identify non-variable stars in each target region, and use their known magnitudes and colours to determine and correct for the colour terms in each image.

IC 5070 cluster membership

- The star forming region IC 5070 (Pelican Nebula) centred at RA = 20:51:00 and DEC = +44:22:00 and is about 1*1deg in size, which is part of the W 80 Hii region alongside NGC 7000 (North American Nebula) .
- This region was found to be at ~ 796 ± 25 pc which identified 395 YSOs in six astrometric groups in the region based on Gaia DR2. Almost all objects were found to be less than 3 Myr old, with a majority younger than 1 Myr.
- **Select criteria using Gaia DR3**
  - ✓ sources within 0.6 degrees of the cluster centre
  - ✓ parallax>0.3 mas and $SNR_{parallax}$>5 and 750 <distance<900 pc
  - ✓ G<18 mag
  - ✓ excluded source with BP − Gmag < −0.2 mag and Gmag − RP < 0.0 mag (white dwarfs and cataclysmic variables)
  - ✓ distance
- Finally, a total of 366 potential cluster members were selected and of 131 have HOYS light curves with at least 100 photometry data points in each of the V, R, and I filters.

Table 1. Properties of the two astrometric groups of young stars in the IC 5070 region, as determined in Froebrich et al. (2024). The columns contain the following information: Group: The group name; d, d^e, d^s: median distance, standard error of the median, rms scatter from the median of the cluster members; $\mu_{\alpha/\delta}, \mu^e_{\alpha/\delta}, \mu^s_{\alpha/\delta}$: median proper motion in RA/DEC, standard error of the median, rms scatter from the median of the cluster members; N: Number of Gaia DR3 selected potential members;

Group	d	d^e	d^s	μ_α	μ^e_α	μ^s_α	μ_δ	μ^e_δ	μ^s_δ	N
	[pc]			[mas/yr]			[mas/yr]			
a	832.4	2.7	33.6	-1.328	0.028	0.347	-3.076	0.026	0.320	252
b	824.7	4.43	36.0	-0.977	0.036	0.294	-4.148	0.041	0.335	114

Sliced Light Curves

- Their aim is to analyse the properties of surface spots over time. HOYS observations in this field begin in 2014, and the light curves were extracted from our database on October 21st, 2022.
- They have dissected (sliced) the V, R, and I light curves into blocks of six months in length, every three months.
- For their analyses, in each slice, they need at least 50 data points in at least two filters to determine the possible period, and at least 50 data points in each filter to measure the peak-to-peak amplitudes.
- therefore at most there are 17 slices (from 16 to 33, ~5 yr) with sufficient data for spot fitting.

Period Identification

- They used four methods: L1Boot, L1Beta, L2Beta, and the generalised Lomb-Scargle (GLS) periodogram to identify period (see the detailed description in Froebrich et al. 2021).
- **How to selection of the best period,**
  - ✓ The four period finding algorithms (L1Boot, L1Beta, L2Beta, and GLS) were applied to the photometry in each slice and filter (V, R, and I), separately.
  - ✓ For L1Boot, L1Beta and L2Beta, candidate periods with a peak periodogram power above 0.15.
  - ✓ The GLS equivalent to this peak periodogram power is the False Alarm Probability (FAP) and FAP below 0.1 as candidate periods.
  - ✓ removed candidate periods identified within one percent of one day and removed any candidate periods that were within one percent of 0.5 d and 20 d as these are near the edges of the period parameter space they investigated.
  - ✓ in at least two filters with a separation of less than 0.05 d

A histogram of all candidate periods for each object in each filter was created. The peak is the period for each filter and the median of these periods from the V, R, and I data has been adopted as the final period, the standard deviation was used as the final period uncertainty of the object.

Rotation Period Distribution

- Our data set contains light curves in V, R, and I for 131 objects. When divided into the six-month slices, 126 objects had sufficient data in one or more slices to search for a period. For 68 objects we detected a period in at least one slice. Of those, 31 objects meet the criteria to determine a final period.

Table 2. Target list of all YSOs investigated in this work. For each object we list our ID number, the J2000 coordinates, proper motions, and parallax from Gaia DR3, the astrometric group it belong to, the effective temperature used for spot fitting, the determined period and its uncertainty, its $K - W2$ colour (discussed in Sect. 5.4), the Gaia DR3 ID number, and the ID number of the object in Froebrich et al. (2021). Objects marked with (*) have no effective temperature reference in Fang et al. (2020) and the median of all astrometric group members were used or 5000 K for bright objects (see details in text).

Object ID	RA [deg]	Dec	μ_α [mas/yr]	μ_δ	Parallax [mas]	Group	T_{eff} [K]	Period [d]	Period error	$K - W2$ [mag]	Gaia DR3 ID	F21 ID
1	312.87736	44.06249	-2.125	-3.563	1.270	a	4250	3.165756	0.000050	0.817	2066866222797779072	9321
2	312.87063	44.07308	-1.824	-2.883	1.212	a	5000*	4.82799	0.00026	0.200	2066866287224242432	9267
3	312.78140	44.17626	-1.870	-3.665	1.162	a	4100*	3.53001	0.00013	0.441	2066870689567848192	8038
4	312.74312	44.24230	-1.198	-4.790	1.308	b	4350	4.87960	0.00028	0.710	2067058740416252416	7422
5	312.74341	44.24562	-1.643	-3.794	1.090	a	3700	3.42336	0.00028	0.789	2067058740416252544	-
6	312.45490	44.17951	-1.991	-3.440	1.209	a	4100*	3.30975	0.00019	0.306	2067061042518587264	8025
7	313.09560	44.01580	-1.460	-3.895	1.181	b	3950*	3.63383	0.00055	0.374	2162929419847388544	9961
8	313.35736	44.17924	-0.815	-2.950	1.217	a	4000	1.4533437	0.0000056	0.230	2162934986124720896	7954
9	313.35268	44.34278	-1.226	-3.110	1.291	a	4000	2.779205	0.000058	0.390	2162941273956895872	6393
10	313.09386	44.23338	-1.234	-3.571	1.219	a	4300	3.00608	0.00023	0.910	2162944916089431168	7472
11	312.82599	44.21893	-1.046	-3.998	1.211	b	3950	7.87849	0.00090	1.292	2162947596149035648	7632
12	312.92257	44.25196	-1.278	-3.644	1.339	b	3800	6.7210	0.0018	1.527	2162949382855434496	-
13	312.94394	44.37256	-1.743	-3.242	1.164	a	3950	2.175035	0.000017	0.261	2162950413647417728	6149
14	313.14528	44.23346	-1.826	-3.406	1.209	a	4200	10.63240	0.00042	0.245	2162950546789495552	7465
15	313.14322	44.29450	-1.116	-3.690	1.216	b	3900	7.27588	0.00066	1.508	2162951753677142784	-
16	313.07438	44.35441	-1.463	-3.256	1.239	a	3950	3.211	0.069	0.071	2162955086571795712	6315
17	313.46770	44.28486	-1.437	-3.392	1.234	a	4950	7.3783	0.0076	0.274	2162960481050791936	-
18	313.42432	44.36014	-0.934	-3.183	1.226	a	4900	1.44775	0.00013	0.174	2162964088823157632	-
20	312.75611	44.25956	-1.208	-3.744	1.171	b	3900	5.523	0.051	1.093	2163135573981345280	-
21	312.75654	44.26166	-1.232	-3.811	1.239	b	4000	7.35691	0.00057	1.633	2163135578281583744	7181
22	312.81307	44.30488	-1.019	-4.277	1.197	b	3950	4.22837	0.00032	1.382	2163136059317926016	6813
23	312.71903	44.27889	-1.215	-4.409	1.267	b	4300	8.311	0.089	1.451	2163136368555566848	-
24	312.74460	44.29188	-0.746	-4.149	1.270	b	3900	7.2272	0.0029	1.124	2163136402915307136	6929
25	312.77764	44.36131	-1.538	-2.702	1.285	a	4750	1.39729	0.00013	0.198	2163137261908777472	6259
26	312.84446	44.35210	-1.062	-4.050	1.198	b	3950	3.882	0.021	1.176	2163137742945115136	6337
27	312.81884	44.38277	-1.213	-2.641	1.176	a	4300	2.4243735	0.0000087	0.485	2163138601938577024	6060
28	312.69199	44.31941	-1.146	-4.597	1.379	b	3500	13.690	0.262	1.200	2163139594070911360	-
29	312.93710	44.43861	-1.235	-3.185	1.172	a	3950	3.77296	0.00011	0.217	2163144271295324544	5559
30	313.10923	44.57394	-1.501	-2.871	1.244	a	5500	1.43272	0.00013	0.234	2163146779556221952	4446
31	312.84503	44.56183	-2.157	-3.099	1.273	a	3950*	4.96447	0.00090	1.023	2163148772421081728	-
32	312.72580	44.63561	-2.087	-2.686	1.241	a	3950	9.5466	0.0030	1.280	2163156056685634944	3988
19	313.36180	44.42429	-1.326	-2.740	1.248	a	4100*	0.6261	0.0034	0.259	2162965252757133056	-

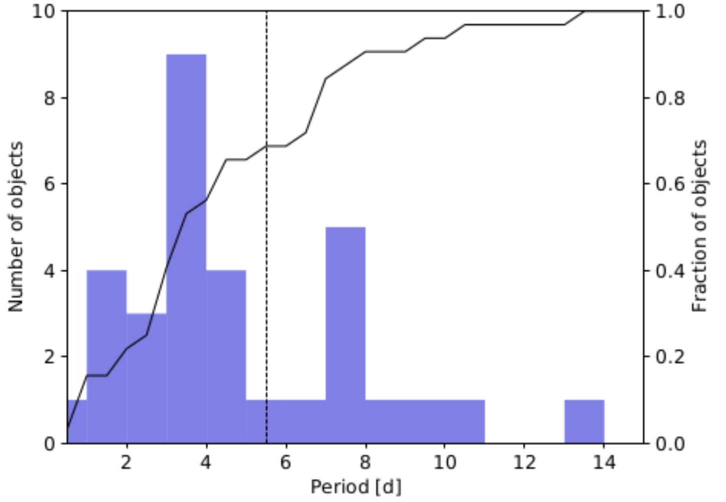

Figure 1. Distribution of measured periods of YSOs in our IC 5070 sample. The solid black line represents the cumulative distribution function. The dashed vertical line placed at a period of 5.5 d separates slow from fast rotators.

23 are found to have P < 5.5 d and 9 have P > 5.5 d. The distribution roughly peaks at ~3 d and ~7 d. The cause of this bimodality is attributed to star-disc interactions via magnetic fields. Long rotation periods are indicating a disc slowing the rotation rate. Conversely, once the disc is dissipated or looses the magnetic connection to the star, the star begins to 'spin up', leading to fast rotators.

Gaia Colour Magnitude Diagram

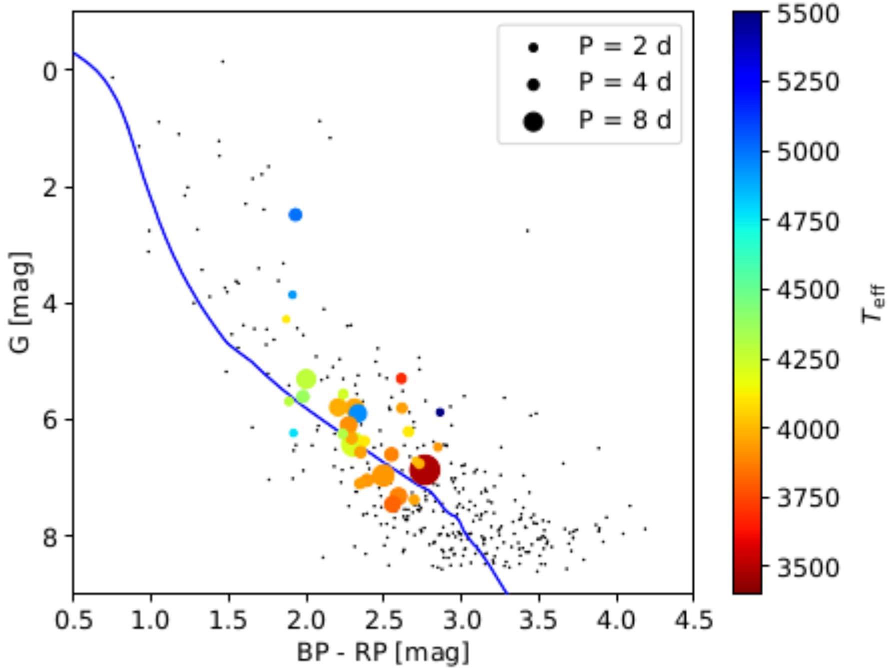

Figure 2. $BP - RP$ vs. G colour magnitude diagram. All selected IC 5070 cluster members as shown as black points and periodic objects are in colour mapped to their effective temperature from Fang et al. (2020), or the sample median. The marker size is scaled to the period, as shown in the legend. Overlaid in blue is a 1 Myr PARSEC isochrone (Bressan et al. 2012).

They find no significant trend between period and colour.

Peak to peak amplitude identification

- In order to analyse the spot property evolution we require peak to peak amplitudes in V, R, and I over time.
- The peak to peak amplitude as A_{λ}^{o} , which is determined as the difference between the maximum and minimum of the smoothed running median brightness in the phase plot.
- The associated uncertainties σ A_{λ}^{o} are determined as the standard error of the mean of the data used.
- They discarded all peak to peak amplitudes in slices in which one or more of them had a SNR below three and discarded when the phase position of the maximum or minimum in the folded light curve scattered by more than 45 degrees between the three filters.

Spot property fitting

- Two assumeitions

a) They assume that the A_λ^o in each six-month slice is generated by a single, uniform spot with temperature T_S on an otherwise unspotted surface with temperature $T_\star$.

b) They assume that the spot rotates completely in and out of the line of sight and therefore consider the spot to be 'in-front' or 'behind' of the star.

- Model

➢ Using a flux replacement model with PHOENIX synthetic spectra, we model for a given stellar temperature T★ (from Fang et al. 2020) , 10^6 spots homogeneously sampled in the spot temperature T_S range of 2000 K $\leq T_S \leq$ 10000 K and spot coverage f range of the visible surface, $0 \leq f \leq 0.5$.

the model peak-to-peak amplitude A_λ^m is

$$\hat{A}_\lambda^m = \left|2.5 \cdot \log\left(\frac{F^\lambda(T_\star)}{(1-f)\cdot F^\lambda(T_\star) + f\cdot F^\lambda(T_S)}\right)\right| \qquad (1)$$

- The best fitting spot for the observations is with the minimum $RMS_{\{\lambda\}}$

$$RMS_{\{\lambda\}} = \sqrt{\frac{1}{N}\sum_{\{\lambda\}}\left(\hat{A}_\lambda^o - \hat{A}_\lambda^m\right)^2} \qquad (2)$$

- This single result will be sensitive to the input peak to peak amplitudes. Thus, the A_λ^o values are varied within their associated uncertainties for 10000 iterations. In the majority of cases there are cold spot and hot spot solutions for the A_λ^o variations. They require at least 60% of the 10000 variations to be either hot or cold spot solutions. The ratio of hot spot to cold spot solutions HS:CS {V } , is used as an indicator of reliability for the solution.

Object Result Summary Plots

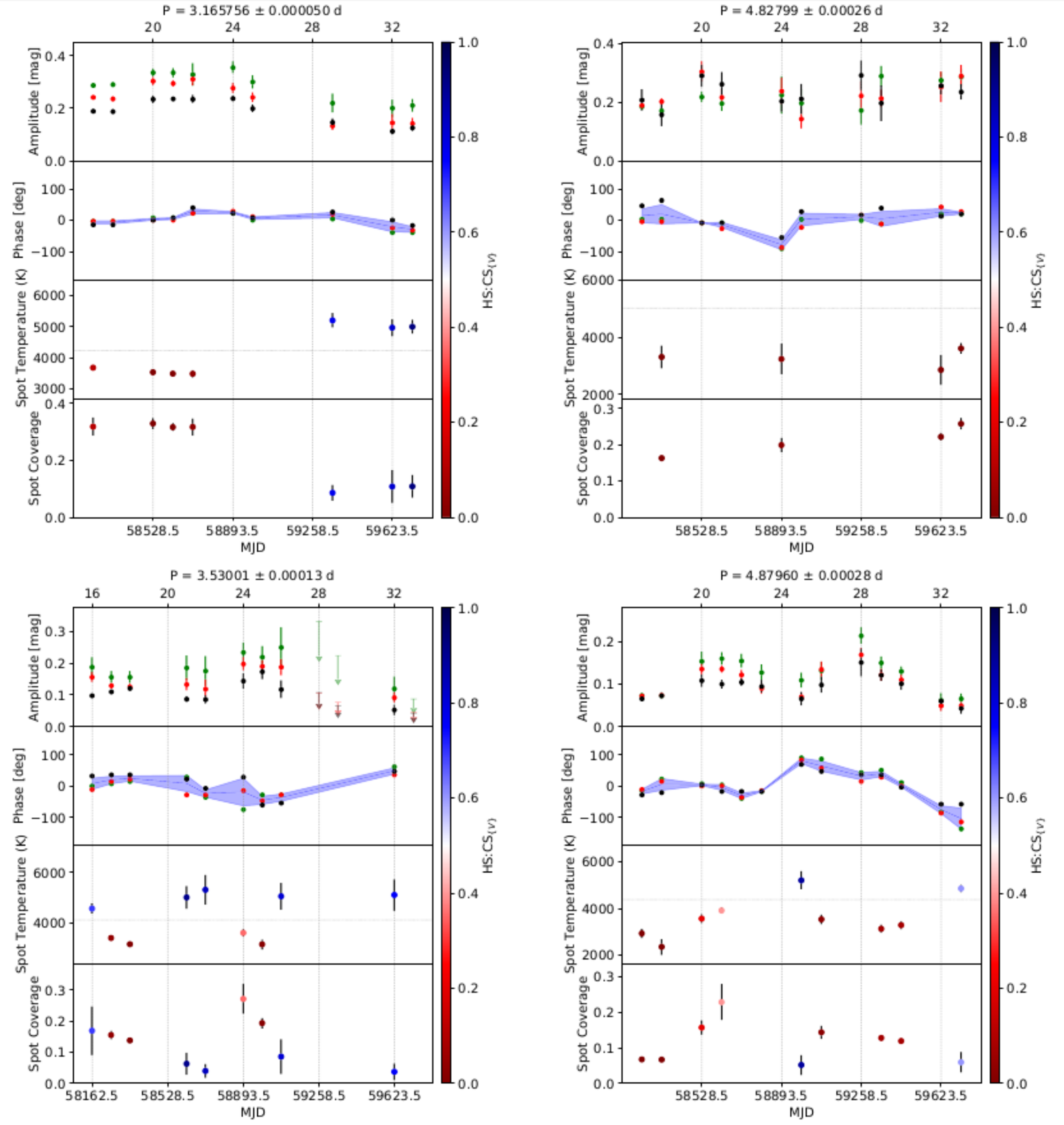

Figure 4. Result summary plots for the first four objects in our sample. The data for object 1 are shown in the top left panel, object 2 in the top right panel, object 3 in the bottom left panel, and object 4 in the bottom right panel. In each of the summary plots we show from top to bottom the peak to peak amplitudes, the maximum brightness phase positions, the determined spot temperatures, and the spot coverage against time. For more details see the description in Sect. 5.1.

The first (top) panel shows the peak to peak amplitude A_V^o (green), A_R^o (red), A_I^o (black) values.

The second panel shows the phase position (in degrees) of the maximum brightness in the phase folded light curve in each filter.

the third panel shows the spot temperatures. The dashed horizontal line indicates the surface temperature of the star

The bottompanel shows the spot coverage.

The colour coding of the symbols in the bottom two panels follows the scale shown at the right hand side of the figure. It represents the ratio of the hot spot to cold spot solutions (HS:CS {V }) during the spot property fitting. Thus, spots that are mostly fitted as cold spots are shown in red, and spots that are mostly classified as hot spots are displayed in blue.

Spot Property Distribution

- In those 234 amplitude sets we can reliably fit 180 as spots. Of these we identify 125 as cold spot solutions and 55 solutions are warm or hot spots.

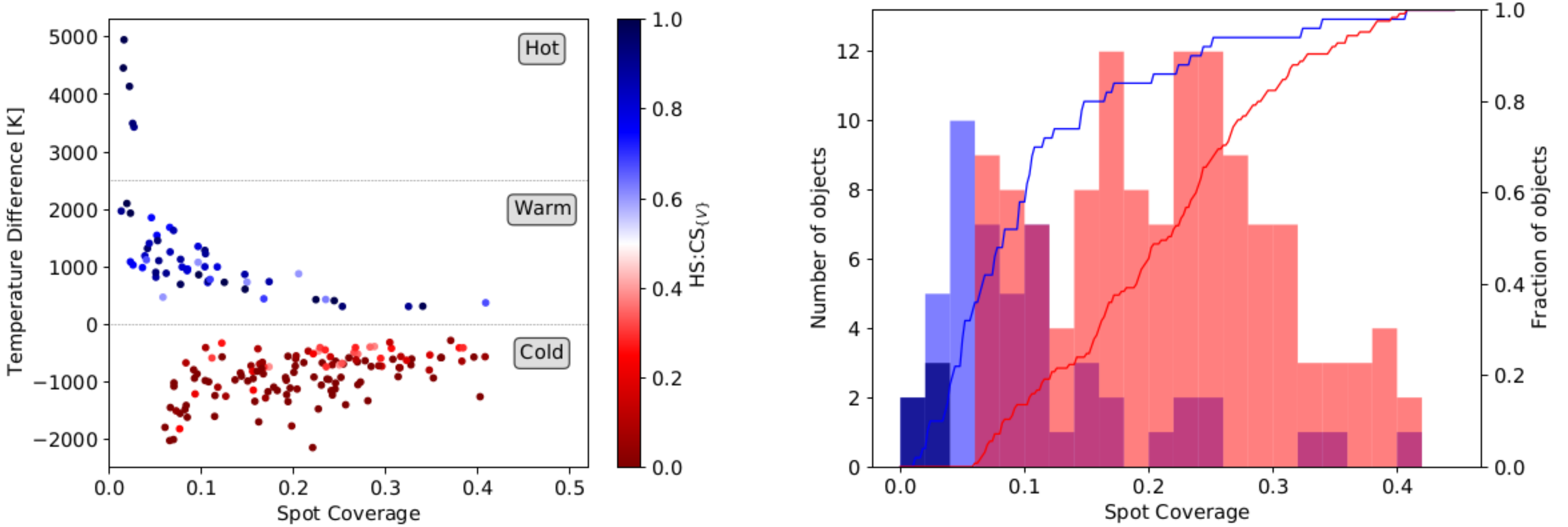

Figure 5. Left: Spot temperature difference $T_S - T_\star$ versus spot coverage. Horizontal dotted lines mark $T_S - T_\star = 0$ K and $T_S - T_\star = 2500$ K, which separate the cold, warm and hot spot solutions. The markers are colour coded according to the HS:CS$_{\{V\}}$ ratio. **Right:** Distribution of spot coverage of hot (dark blue), warm (blue), and cold spots (red). The solid lines are the CDFs of the warm (blue) and the cold spots (red).

Rapidly changing spot properties

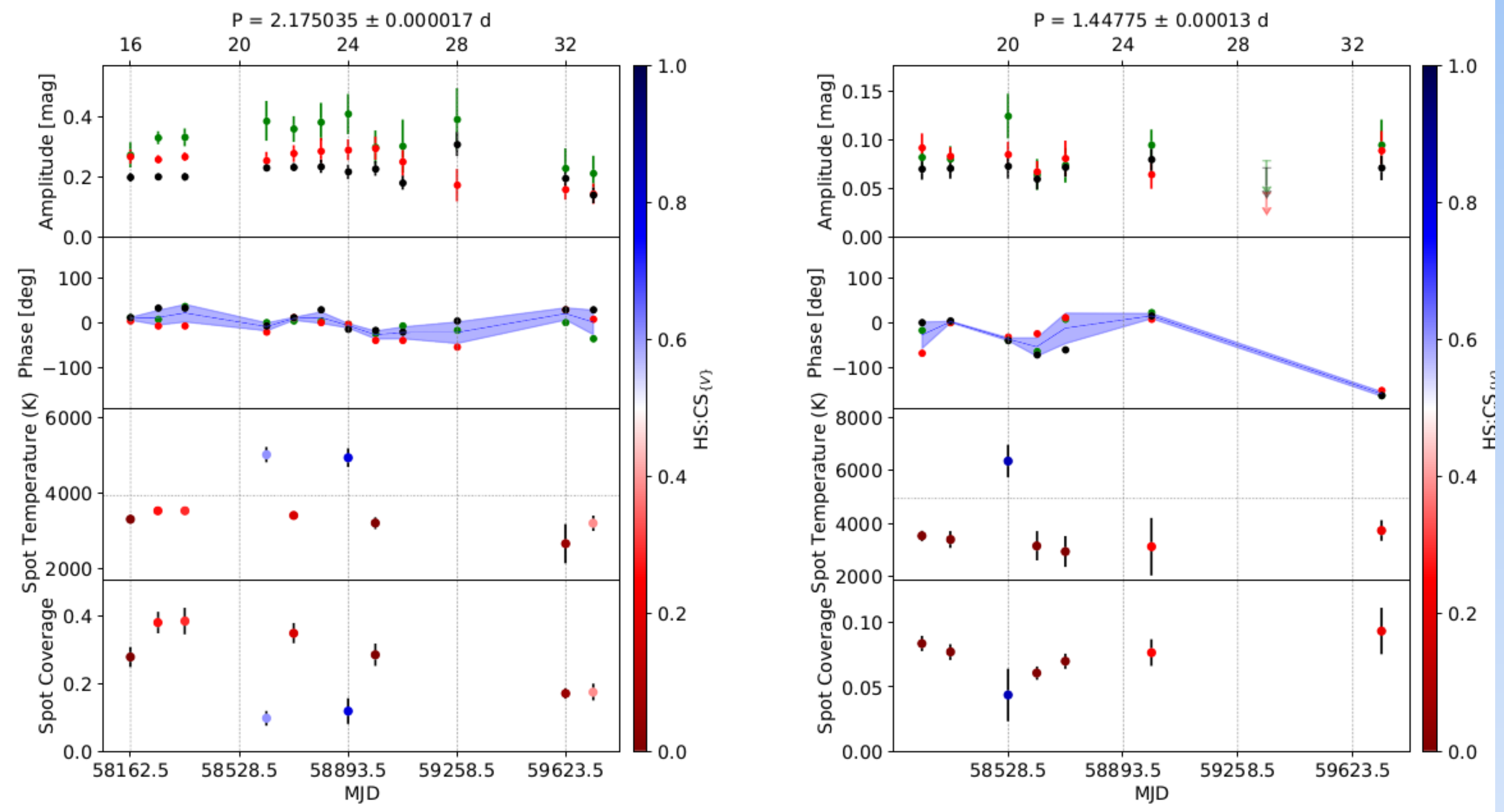

Figure 6. As Fig. 4, but for the objects 13 (left) and 18 (right).

A small hot spot can make a significant contribution to the peak to peak amplitudes. In the 180 d long slices used here, the asymmetric part of the spot distribution on the stars can evolve. Thus, evolving spots will most likely lead to HS:CS $_{\{V\}}$ values changing or moving into the range where no clear solution can be found.

Stellar Rotation Periods and Disc Excess Emission

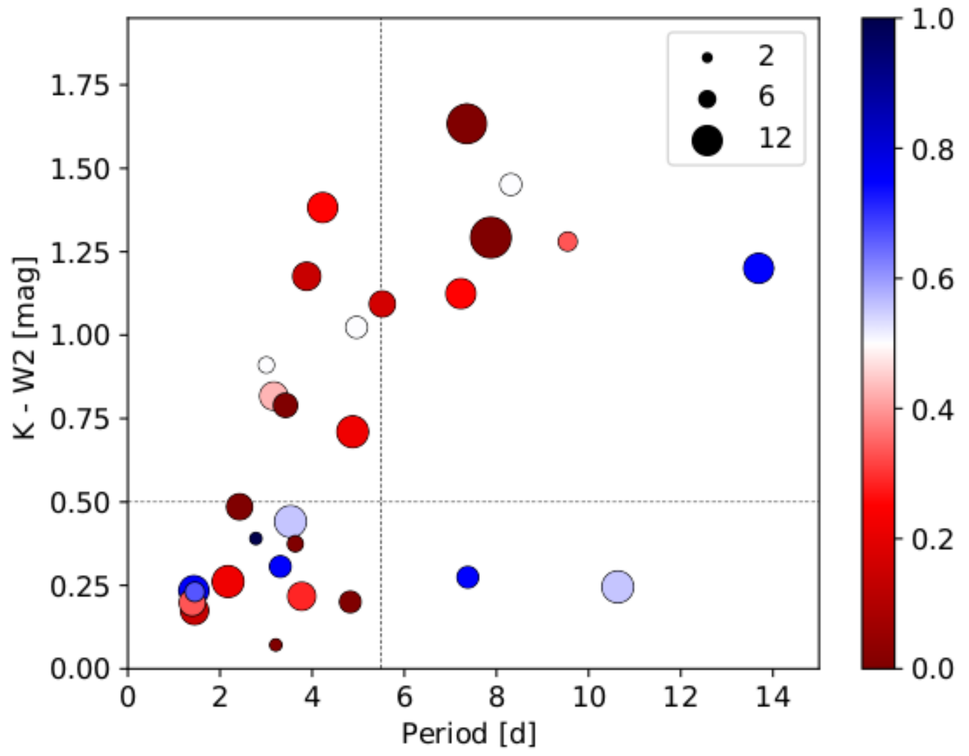

Figure 7. Period against $K - W2$ for our objects. The horizontal dashed line separates objects with a detectable inner disc (above) from sources without (below). The vertical dashed line separates fast and slow rotators. Markers are coloured based on the proportion of warm/hot spot measurements on them, according to the colour scale on the right. Values of zero (dark red) indicate that all spot solutions are cold, values of one (dark blue) mean all spot solutions are warm/hot. The marker size is scaled to number of spot property measurements, as shown in the legend.

A horizontal dashed line at K −W2 = 0.5 mag (Teixeira et al. 2012) which separates sources with a detectable warm inner disc (above) and without (below). 15 objects of our sample do not show a disc excess emission and 14 objects do.

Observations at longer wavelengths can be used to probe the presence of disc material further from the star. There are 17 objects, however, that have a better than 5σ detection in all four WISE filters. They determine the slope of the spectral energy distribution (α SED) following (Majaess 2013) for all of these. They find that amongst the 17 objects, one is classified as a Class 1 protostar (28), 15 are Class 2 objects, and one (7) is a Class 3 source.

A longer period may indicate that the central star still has magnetic ties to the inner disc, slowing rotation. Faster rotators have been spinning up due to a lack of this disc-breaking mechanism (Herbst et al. 2007). There is a loose positive correlation of the rotation period and disc excess emission,

Causes of the Surface Spots

- **cold spots:** 70 percent of our reliable spot solutions. The presence of these cold spots on young stars is well understood as being caused by magnetic activity on the stellar surfaces, driven by the rotation of the stars (Herbst et al. (2007) and Bouvier et al. (2014)). These spots are known to have a range of temperatures and can reach up to half the visible surface.

- **warm/hot spot:** Eight warm/hot spot dominated objects. Only one of these has a detectable inner disc (28).

    a) Accretion is common over an inner disc gap, although whether the rate is equivalent with full disc object is subject to debate, and so these warm/hot spots may be accretion related features.

    b) Alternatively, warm photospheric plages have been observed on WTTSs with coverage values of around six percent. (These are presumed to be caused by mass flow between the regions of opposing polarities.)

So, the low coverage warm spots may be accretion related warm regions or plages, whereas the larger regions are more likely accretion related.

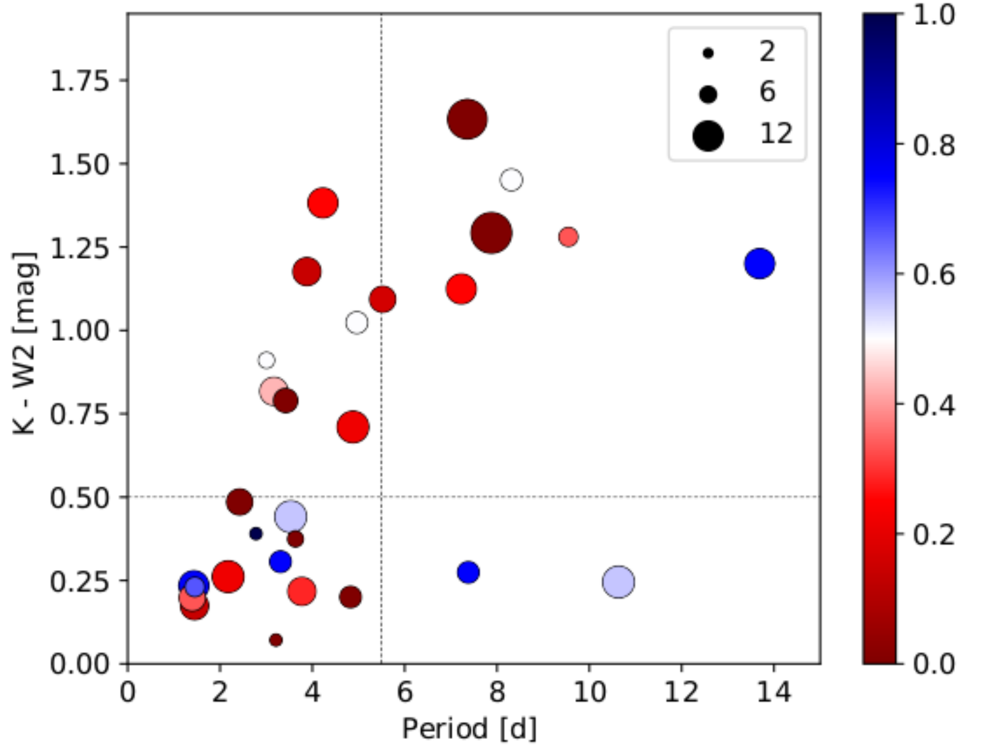

Figure 7. Period against $K - W2$ for our objects. The horizontal dashed line separates objects with a detectable inner disc (above) from sources without (below). The vertical dashed line separates fast and slow rotators. Markers are coloured based on the proportion of warm/hot spot measurements on them, according to the colour scale on the right. Values of zero (dark red) indicate that all spot solutions are cold, values of one (dark blue) mean all spot solutions are warm/hot. The marker size is scaled to number of spot property measurements, as shown in the legend.

Conclusions

- Froebrich et al. (2024) identified 366 YSOs in IC 5070 from Gaia DR3 data. Of these, 131 have light curves with at least 100 data points in V, R, and I from the HOYS.
- They have used the peak to peak amplitudes in V, R, and I to measure spot properties. Out of the 234 amplitude sets, we find 180 reliable spot solutions.
- They measured a wide range of spot properties. Roughly two thirds of all reliable spot solutions are cold. They suggest a limit at 2500 K above the stellar temperature, separating warm and hot spots.
- They find five hot spot solutions that are ~3000 K above the stellar temperature, with coverage values of less than three percent.
- The entire YSO sample has an inner disc fraction of about 50 percent, based on the $K - W2$ infrared excess.
- We find that objects with more reliable spot solutions overall tend to have a higher proportion of cold spot solutions. Warm/hot spot dominated objects tend to have fewer reliable spot solutions. This implies that cold spots are longer lived, or more likely to produce rotational variability over longer timescales.
- The low coverage warm spots may be accretion related warm regions or plages, whereas the larger regions are more likely accretion related.

Thanks!